arXiv:nucl-th/0011008 2 Nov 2000

σ Exchange in the NN Interaction within the Chiral Unitary Approach

E. Oset[1,2], H. Toki[1], M. Mizobe[1] and T. T. Takahashi[1]

[1] *Research Center for Nuclear Physics(RCNP), Osaka University*
Mihogaoka 10-1, Ibaraki, Osaka 567-0047, Japan
[2] *Departamento de Física Teórica and IFIC, Centro Mixto Universidad de Valencia-CSIC, 46100 Burjassot (Valencia), Spain*

November 6, 2000

Abstract

We study the nucleon-nucleon interaction in the isoscalar-scalar channel using the chiral unitary approach. The t-matrix of the pion-pion scattering in this channel is summed up to all orders using the B-S equation. We find that the calculated results at long distances are close to those of the σ-exchange interaction. In addition, there appears a shorter range repulsion in this channel.

1 Introduction

The intermediate range attraction in the NN interaction has been traditionally described by the σ-exchange in the meson exchange picture. [1] It has also been noticed [2, 3, 4] that box diagrams with two-pion exchange and intermediate Δ excitation lead to an intermediate range attraction. A weakened σ exchange together with these box diagrams has also been used to describe the intermediate range NN attraction. [1]

With the success of chiral perturbation theory (χPT) in the meson-meson and meson-baryon sectors, [5] attempts to extend these ideas to the NN sector have been

pursued. [6, 7, 8] In a recent paper, [9] following the line of Ref. [8], the peripheral NN partial waves are studied within a chiral scheme, using the meson-meson and the meson-baryon interaction Lagrangians. With this input, together with more conventional processes with Δ box diagrams, ρ exchange and other meson exchange, a good reproduction of the NN data for $L > 2$ partial waves is obtained.

A striking feature of Ref. [9] is that the exchange of two interacting pions in the scalar-isoscalar channel (the σ channel) leads to a repulsion (although weak), instead of the commonly accepted attraction from σ exchange. Simultaneously, from the box diagrams with intermediate Δ, an attraction is obtained with the range and strength of the standard σ exchange of the boson exchange models. Two basic approximations lead to these results. First, the $\pi\pi$ isoscalar interaction is used only to lowest order in χPT. Second, no form factors are considered for the Δ box diagrams.

In the present work we wish to reconsider this idea and go further by treating the exchange of two interacting pions in the isoscalar channel in a nonperturbative way. The approach followed here for the $\pi\pi$ interaction produces a σ pole in the complex plane in the physical region $s > 4m_\pi^2$. Then the analytical extrapolation of the model is used in order to find the strength of the isoscalar exchange interaction for the situation $s < 0$, which one encounters in the NN scattering problem.

The σ meson has been rather problematic, with ups and downs in the particle data tables, where it has been once again welcome. [10] Some analyses of the $\pi\pi$ data rely on the σ pole in the $\pi\pi$ t matrix. [11, 12, 13] Theoretical models for the $\pi\pi$ interaction based on meson exchange [14] find also a pole in the t matrix for the σ meson. Yet, of relevance to the present work is the fact that the σ pole is found in recent chiral nonpertubative approaches which have developed independently. [15, 16] In Ref. [15] the inverse amplitude method using the lowest order and second order chiral Lagrangians is formulated and it leads to a pole position for σ at $440 - i245$ MeV. In Ref. [16] the Bethe Salpeter equation, with a cutoff in the loops fitted to the data of the scalar sector, is shown to reproduce accurately the data in the scalar sector up to around $\sqrt{s} = 1.2$ GeV, using only the lowest order chiral Lagrangian as input. In this case, σ appears as a pole at $469 - i203$ MeV [Ref. [16],erratum]. The approach of Ref. [16], using coupled channels, is able to reproduce the σ and f_0 (980) resonance in the scalar-isoscalar sector and the $a_0(980)$ resonance at $L = 0$, $I = 1$. The approach of Ref. [15] using only the $\pi\pi$ channel could only generate σ in the scalar channel, but ρ and K^* in the vector channel were accurately reproduced.

A generalization of the inverse amplitude method of Ref. [15], incorporating coupled channels as in Ref. [16] and using the lowest and second order chiral La-

grangians, is given in Ref. [17], and there, all meson-meson data up to $\sqrt{s} = 1.2$ GeV are accurately reproduced. In the latter work, the σ pole appears at $442 - i225$ MeV.

A different chiral approach is employed in Ref. [18], using the N/D method. This explicitly intoduces resonances on top of the lowest order chiral Lagrangian. That approach, which includes contributions from the physical and unphysical cuts through dispersion relations, produces good results up to $\sqrt{s} = 1.4$ GeV and also leads to a σ pole at $445 - i221$ MeV.

As we can see, all these different schemes, which uses the lowest order chiral Lagrangian and the implementation of exact unitarity, lead invariably to a σ pole around $450 - i225$ MeV, with small fluctuations.

Our aim here is to follow these lines and use the unitary scheme to generate the $\pi\pi$ scalar isoscalar amplitude in the unphysical (virtual) region, and later its contribution to the NN interaction.

2 Lowest order contribution in isoscalar exchange in the NN interaction

We first investigate the lowest-order contribution to the $\pi\pi$ interaction in the scalar isoscalar channel, which is given by the diagrams of Fig. 1 for $pp \to pp$. We leave out the box diagram contribution here and just refer the literature. [1]

Considering the $\vec{\tau}\ \vec{\phi}$ isospin dependence of the πNN coupling, one gets from the sum of the diagrams in Fig.1 the combination,

$$t_{\pi^0\pi^0\to\pi^0\pi^0} + 2t_{\pi^0\pi^0\to\pi^+\pi^-} + 2t_{\pi^+\pi^-\to\pi^0\pi^0} + 4t_{\pi^+\pi^-\to\pi^+\pi^-}. \tag{1}$$

Taking into account the unitary normalization of the $\pi\pi$ states of Ref. [16],

$$|\pi\pi, I = 0\rangle = -\frac{1}{\sqrt{6}}|\pi^0\pi^0 + \pi^+\pi^- + \pi^-\pi^+\rangle, \tag{2}$$

the combination of t-matrices in Eq. (1) corresponds, in terms of the isoscalar $\pi\pi$ amplitude, to

$$6t^{(I=0)}_{\pi\pi\to\pi\pi}. \tag{3}$$

We should note here that all the pion lines in Fig. 1 are off shell, which requires the use of the off shell t-matrix. From Ref. [16] this off shell amplitude obtained from

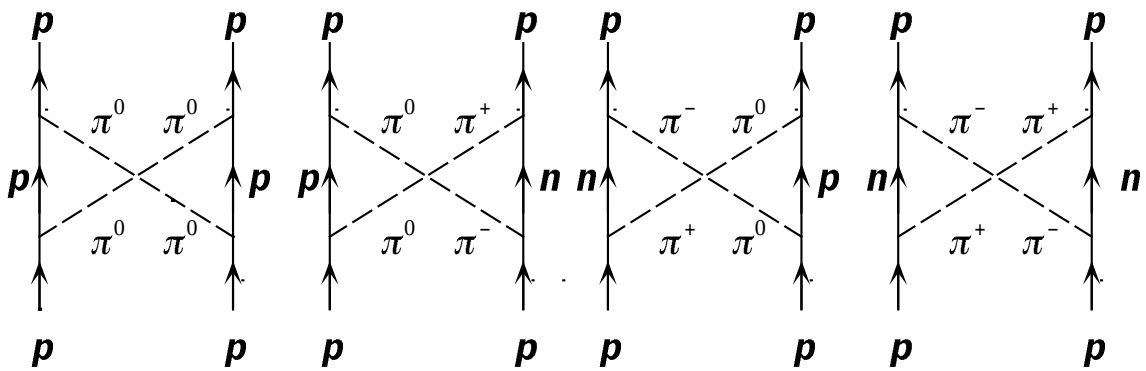

Figure 1: The lowest-order processes in the $\pi\pi$ interaction in the scalar isoscalar channel for pp$\to$pp

the lowest order meson-meson Lagrangian is given by

$$t^{(I=0,L)}_{\pi\pi\to\pi\pi} = -\frac{1}{9f^2}\left(9s + \frac{15m_\pi^2}{2} - 3\sum_i p_i^2\right), \tag{4}$$

where f is the pion decay constant ($f = 93$ MeV), s is the $\pi\pi$ Mandelstam variable, and the p_i are the momenta of the pion lines. We define the on-shell value of the amplitude as that of Eq. (4) when $p_i^2 = m_\pi^2$. This allows us to write in a convenient way

$$t^{(I=0,L)}_{\pi\pi\to\pi\pi} = t^{(I=0,L,OS)}_{\pi\pi\to\pi\pi} + \frac{1}{3f^2}\sum_i (p_i^2 - m_\pi^2), \tag{5}$$

with the on shell value of the amplitude

$$t^{(I=0,L,OS)}_{\pi\pi\to\pi\pi} = -\frac{1}{f^2}\left(s - \frac{m_\pi^2}{2}\right). \tag{6}$$

In what follows we prove that the off shell contribution of the amplitude, i.e., the terms proportional to $p_i^2 - m_\pi^2$, cancels exactly with the diagrams of Fig. 2,

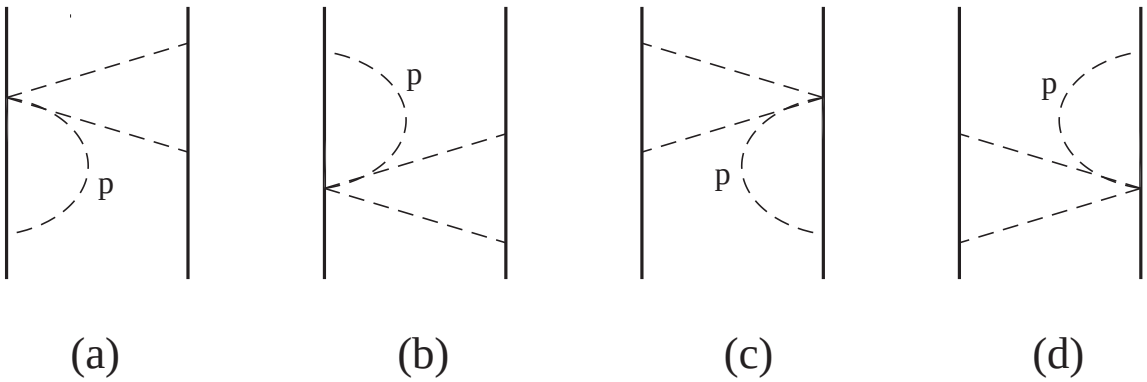

Figure 2: The processes with three meson vertex at a baryon line for $pp \to pp$.

which appear at the same order of the chiral counting. The diagrams of Fig. 2 contain the vertices with one baryon line and three mesons. The baryon-meson chiral Lagrangian relates this function to that with one meson attached to the baryon line. This interaction term is given by [19]

$$\mathcal{L}_1^{(B)} = \frac{D+F}{2}(\bar{p}\gamma^\mu\gamma_5 u_\mu^{11} p + \bar{n}\gamma^\mu\gamma_5 u_\mu^{22} n + \bar{n}\gamma^\mu\gamma_5 u_\mu^{21} p + \bar{p}\gamma^\mu\gamma_5 u_\mu^{12} n) \tag{7}$$

where p and n represent the proton or neutron fields. In Eq. (7) u_μ is the $SU(2)$ matrix given by

$$u_\mu = -\frac{\sqrt{2}}{f}\partial_\mu\Phi + \frac{\sqrt{2}}{12f^3}(\partial_\mu\Phi\Phi^2 - 2\Phi\partial_\mu\Phi\Phi + \Phi^2\partial_\mu\Phi), \tag{8}$$

and Φ is the $SU(2)$ matrix for the pions given by

$$\Phi = \begin{pmatrix} \frac{1}{\sqrt{2}}\pi^0 & \pi^+ \\ \pi^- & -\frac{1}{\sqrt{2}}\pi^0 \end{pmatrix}. \tag{9}$$

Equation(7), with the first term of u_μ in Eq. (8) gives rise to the πNN coupling, which in the nonrelativistic reduction, $\gamma^\mu\gamma_5 \to \sigma^k\delta_{\mu k}$, reads

$$\begin{aligned} -it_{\pi^i NN} &= C_i\frac{D+F}{2f}\vec{\sigma}\cdot\vec{p}, \\ C_{\pi^+} &= C_{\pi^-} = \sqrt{2};\ C_{\pi^0 pp} = 1;\ C_{\pi^0 nn} = -1 \end{aligned} \tag{10}$$

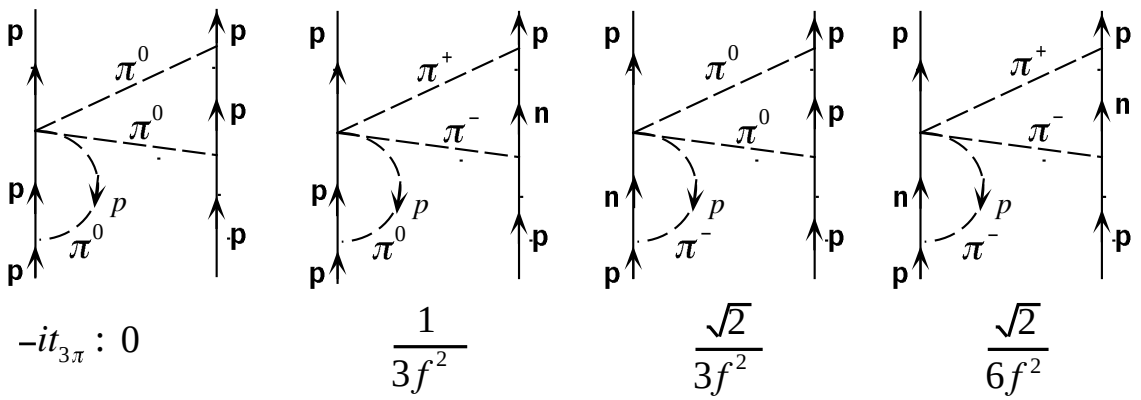

Figure 3: Diagrams involving the three pion vertex. The figure displays the coefficient which multiplies $\frac{D+F}{2f}\vec{\sigma}\vec{p}$ for each three pion vertex.

for incoming pion with momentum $\vec{p}$.

The second term in the expansion of u_μ gives rise to the three pion vertices and involves derivatives in the three pion fields. However, given the fact that the πNN vertex in the loops with meson momentum p of Fig. 2 contain the p-wave coupling $\vec{\sigma}\vec{p}$, only the term which involves the derivative in the pion with momentum p, which will give rise to another $\vec{\sigma}\vec{p}$ vertex, will contribute in the loop integration. In Fig. 3 we show the diagrams corresponding to the loop in Fig. 2(a) for the different isospin combinations of Fig. 1, together with the contribution of the three meson vertex to each diagram.

If one sums the contributions of all the diagrams in Fig. 3 including the isospin weight of the πNN vertices one obtains an equivalent three pion vertex,

$$-it_{3\pi} \equiv \frac{1}{3f^2}\frac{D+F}{2f}\vec{\sigma}\cdot\vec{p}\,(2+2+2) = \frac{6}{3f^2}\frac{D+F}{2f}\vec{\sigma}\cdot\vec{p}. \tag{11}$$

Now let q be the momentum exchanged between the protons and let us evaluate the diagrams of Fig. 1 with the off shell part of the meson-meson vertex and the diagrams of Fig. 3. We present them in Fig. 4 with the appropriate momentum assignment.

The loops to the right in both diagrams of the figure are the same. Hence, we concentrate only on the loop of the left. Let us pick up the term $((p+q)^2 - m_\pi^2)/3f^2$

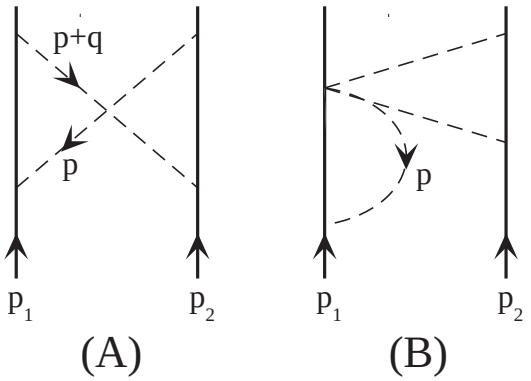

Figure 4: Diagrams where off-shell cancellations appear. Diagram (A) with the off shell part of the $\pi\ \pi$ amplitude from the line $p+q$ cancels diagram (B).

of the meson-meson vertex, which provides the off shell contribution of the left top meson in diagram (A). We then get

$$V^{(A)} = i\left(\frac{D+F}{2f}\right)^2 \int \frac{d^4p}{(2\pi)^4}\vec{\sigma}\cdot(\vec{p}+\vec{q})\vec{\sigma}\cdot\vec{p}\ 6\frac{1}{3f^2}[(p+q)^2-m_\pi^2]\frac{1}{p^2-m_\pi^2+i\epsilon} \frac{1}{(p+q)^2-m_\pi^2+i\epsilon}\ \frac{M}{E(\vec{p_1}+\vec{p})}\ \frac{1}{p_1^0+p^0-E(\vec{p_1}+\vec{p})+i\epsilon}, \quad (12)$$

with M and E the mass and on shell energy of the nucleon. Similarly, we obtain the contribution from the loop on the left in diagram (B),

$$V^{(B)} = -i\left(\frac{D+F}{2f}\right)^2 \int \frac{d^4p}{(2\pi)^4}\vec{\sigma}\cdot\vec{p}\ \vec{\sigma}\cdot\vec{p}\ 6\frac{1}{3f^2}\ \frac{1}{p^2-m_{\pi^2}+i\epsilon} \frac{M}{E(\vec{p_1}+\vec{p})}\ \frac{1}{p_1^0+p^0-E(\vec{p_1}+\vec{p})+i\epsilon}. \quad (13)$$

In Eq. (12) one can see a cancellation of the off-shell part of the meson-meson vertex with the corresponding meson propagator. The rest of the integrand only contains q in the term $\vec{\sigma}\cdot\vec{q}\ \vec{\sigma}\cdot\vec{p}$. This term vanishes exactly in the limit $\vec{p_1}\to 0$, or in any case if one makes the heavy baryon approximation ${p_1}^0 - E(\vec{p_1}+\vec{p}) = 0$. (The corrections are of order $(\vec{p_1}/M)^2$, which we can neglect.) We shall evaluate the NN potential

for $\vec{p_1} = 0$ for simplicity. With the $\vec{\sigma} \cdot \vec{q}\ \vec{\sigma} \cdot \vec{p}$ term of Eq. (12) vanishing, we observe that $V^{(A)}$ and $V^{(B)}$ are equal but with opposite sign, and hence there is an exact cancellation of these two terms.

If now we take the off shell part of the meson vertex corresponding to the other mesons we would observe an exact cancellation with the diagrams (b)-(d) of Fig. 2. This is interesting for practical purposes since it means at the end that we must evaluate only the diagrams of Fig. 1 and using only the on-shell value of the meson-meson vertex.

The need to include this subset of chiral diagrams to find cancellations in the NN isoscalar interaction was already stressed in Ref. [9]. There, different arguments were used, recalling that in the expansion of the pion field matrix $U(\vec{\pi})$, the third order term has ambiguities and the result cannot depend upon them. The on-shell amplitude does not depend on these ambiguities, so here we also prove that, after summing the terms discussed above, the results do not depend on unknown parameters which would affect the off shell meson-meson amplitude.

The derivation here is particularly useful for our purposes, since in Ref. 16) it was also shown that in the construction of the full meson-meson amplitude, only the on-shell part of the meson-meson vertex was needed. This allows us to sum immediately the set of diagrams that were included in the unitary Bethe-Salpeter approach to the scalar meson amplitude and, hence, in the NN interaction we would have the set of diagrams shown in Fig. 5.

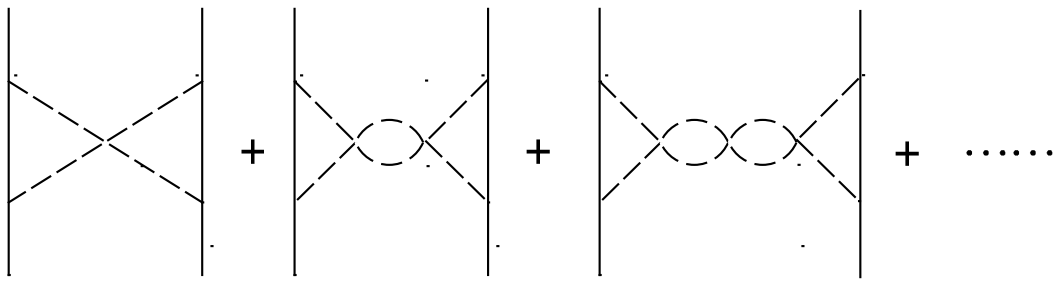

Figure 5: The nucleon-nucleon interaction in the scalar-isoscalar channel, where the $\pi\pi$ scattering t-matrix is summed up to all orders in the unitary approach.

3 Unitary approach for the interacting pions in the isoscalar chnnel

The diagrams of Fig. 5 are easily summed up. First one must substitute the on-shell lowest-order meson-meson amplitude of Eq. (6) with the Bethe-Salpeter amplitude, [16]

$$t^{(I=0)}_{\pi\pi\to\pi\pi} = -\frac{1}{f^2}\frac{(s-\frac{{m_\pi}^2}{2})}{1+\frac{1}{f^2}(s-\frac{{m_\pi}^2}{2})G(s)}. \tag{14}$$

The function $G(s)$ is the loop function with two pion propagators,

$$G(s) = i\int\frac{d^4q}{(2\pi)^4}\frac{1}{{q^2-m_\pi}^2+i\epsilon}\ \frac{1}{{(P-q)^2-m_\pi}^2+i\epsilon}, \tag{15}$$

where P is the total momentum of the two-pion system and $P^2 = s$. In Ref. [16] the integral in Eq. (15) was regularized with a cut-off in the CM frame of the two mesons. Here it is better to work in the CM of the two nucleons, and hence an invariant form for $G(s)$ is preferable. This can be done by using the results for $G(s)$ obtained with dimensional regularization, which are shown in Appendix A of Ref. [20] to be equivalent to those of a cut-off. We then have

$$G(s) = \frac{1}{(4\pi)^2}\left[-1+\ln\frac{{m_\pi}^2}{\mu^2}+\sigma\ln\frac{\sigma+1}{\sigma-1}\right], \tag{16}$$

with μ the regularization mass, which was found to be $\mu = 1.2q_{\rm max} = 1.1$ GeV for the value of the cutoff, $q_{\rm max}$, needed for a good fit to the data with the B-S equation and the lowest order χPT as the kernel of the equation. In Eq. (16) the magnitude of σ is

$$\sigma = \sqrt{1-\frac{4{m_\pi}^2}{s}}, \tag{17}$$

In the range $0 < s < 4{m_\pi}^2$, one has an analytical extrapolation which leads to

$$\sigma\ln\frac{\sigma+1}{\sigma-1} \to (\pi-2\alpha)\sqrt{\frac{4{m_\pi}^2}{s}-1};\ \alpha = \arctan\sqrt{\frac{4{m_\pi}^2}{s}-1}, \tag{18}$$

and for $s > 4{m_\pi}^2$ the log of Eq. (16) develops a negative imaginary part. For $s < 0$, σ is always larger than 1, and the log term behaves smoothly.

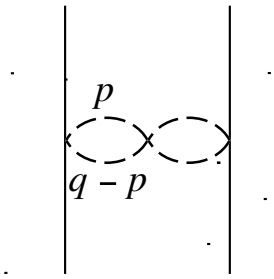

Figure 6: The nucleon-nucleon interaction with the two-pion nucleon vertex in the isoscalar channel.

We would also like to note that at the same order as calculated in this section there are other pieces, like in Fig. 6. The $BBMM$ contact term is proportional to $\gamma^\mu \tau^a$, which implies vector and iso-vector exchange in the t channel, and hence we do not have to consider it for the isoscalar exchange channel we are concerned with here.

In the NN CM frame we have the momentum q exchanged between the nucleons with $q \equiv (0, \vec{q})$, such that $s = -\vec{q}^{\,2}$. The NN potential corresponding to the isoscalar 2π exchange of Fig. 5 then becomes

$$t_{NN}(q) = \widetilde{V}_N^2(q) \frac{6}{f^2} \frac{(\vec{q}^{\,2} + \frac{{m_\pi}^2}{2})}{1 - G(-\vec{q}^{\,2}) \frac{1}{f^2}(\vec{q}^{\,2} + \frac{{m_\pi}^2}{2})}. \tag{19}$$

Here $\widetilde{V}(q)$ is the vertex corresponding to the triangle loop to the left in Fig. 4, which in the limit $\vec{p_1} \to 0$ can be written as

$$\begin{aligned} \widetilde{V}_N(q) &= i \int \frac{d^4p}{(2\pi)^4} \left(\frac{D+F}{2f} \right)^2 \vec{\sigma} \cdot (\vec{p} + \vec{q}) \vec{\sigma} \cdot \vec{p} \, \frac{1}{p^2 - {m_\pi}^2 + i\epsilon} \, \frac{1}{(p+q)^2 - {m_\pi}^2 + i\epsilon} \\ &\quad \frac{M}{E(\vec{p})} \, \frac{1}{M + p^0 - E(\vec{p}) + i\epsilon}. \end{aligned} \tag{20}$$

With the sums over the spins of the intermediate nucleon in the loop we have

$$\vec{\sigma} \cdot (\vec{p} + \vec{q}) \vec{\sigma} \cdot \vec{p} = (\vec{p} + \vec{q}) \cdot \vec{p} + (\vec{q} \times \vec{p}) \cdot \vec{\sigma}, \tag{21}$$

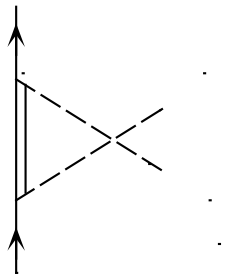

Figure 7: The two pion exchange triangle vertex through delta excitation.

but the integral over $\vec{p}$ in Eq. (20) leads to a vector proportional to $\vec{q}$, which makes the term with $\vec{\sigma}$ of Eq. (21) vanish in the integral. Furthermore, the p^0 integration in Eq. (20) can be done analytically, and one finds

$$\begin{aligned}\widetilde{V}_N(q) &= \int \frac{d^3p}{(2\pi)^3}\left(\frac{D+F}{2f}\right)^2 (\vec{p}^{\,2}+\vec{p}\cdot\vec{q})\frac{M}{E}\,\frac{1}{2}\,\frac{1}{\omega}\,\frac{1}{\omega'}\,\frac{1}{\omega+\omega'} \\ &\quad \frac{1}{E+\omega-M}\,\frac{1}{E+\omega'-M}[\omega+\omega'+E-M], \end{aligned} \tag{22}$$

with

$$E = E(\vec{p});\ \omega = \sqrt{m_\pi{}^2+\vec{p}^{\,2}};\ \omega' = \sqrt{m_\pi{}^2+(\vec{p}+\vec{q})^{\,2}}, \tag{23}$$

The integral in Eq. (22) is logarithmically divergent.

It is straighforward to include the contribution with an intermediate Δ instead of a nucleon in the vertex function, as depicted in Fig. 7. It can be evaluated in a straighforward way, substituting S_iT_j for $\sigma_i\tau_j$ with S and T the spin and isospin transition operators.

The inclusion of the Δ in the fermionic loops is required in order to satisfy the basic rules in the large N_c limit, [21] and we include it here. We obtain

$$\begin{aligned}\widetilde{V}_\Delta(q) &= \frac{4}{9}\left(\frac{f^*_{\pi N\Delta}}{f_{\pi NN}}\right)^2 \int \frac{d^3p}{(2\pi)^3}\left(\frac{D+F}{2f}\right)^2 (\vec{p}^{\,2}+\vec{p}\cdot\vec{q})\frac{M_\Delta}{E_\Delta}\frac{1}{2}\frac{1}{\omega}\frac{1}{\omega'} \\ &\quad \frac{1}{\omega+\omega'}\,\frac{1}{E_\Delta+\omega-M}\,\frac{1}{E_\Delta+\omega'-M}[\omega+\omega'+E_\Delta-M], \end{aligned} \tag{24}$$

with M_Δ the Δ mass and $E_\Delta = ({M_\Delta}^2 + \vec{p}^{\,2})^{1/2}$. We take the empirical value for the ratio of the couplings $f^*_{\pi N\Delta}$ to $f_{\pi NN}$ as 2.12 .

The integral of Eq. (24) is also logarithmically divergent. In order to regularize the integrals of Eqs. (22) and (24), one needs a cutoff or a form factor. Within a quark model one finds natural form factors due to the finite size of the nucleon, but one must still sum over excited states of the quarks in the intermediate states, which leads to a divergence in spite of the form factors. [22] The regularization of the loop in this case can be accomplished by a cutoff in the space of intermediate states, together with a form factor. The truncation at Δ, together with the use of monopole form factors with Λ of order 1 GeV has been found to be a sensible regularization procedure, as proved by the success of such an approach in the cloudy bag model. [23] We shall use here static form factors to keep the p^0 integral of Eq. (20) simple, and hence we include in the integrand of Eqs. (22) and (24) the product of form factors

$$F(\vec{p})F(\vec{p}+\vec{q}) = \frac{\Lambda^2}{\Lambda^2 + \vec{p}^{\,2}} \; \frac{\Lambda^2}{\Lambda^2 + (\vec{p}+\vec{q})^{\,2}}, \tag{25}$$

with $\Lambda \approx 1 - 1.2$ GeV. [1]

Our final form for the NN potential in momentum space is thus given by

$$t_{NN}(q) = \widetilde{V}(q)^2 \frac{6}{f^2} \; \frac{(\vec{q}^{\,2} + \frac{{m_\pi}^2}{2})}{1 - G(-\vec{q}^{\,2})\frac{1}{f^2}(\vec{q}^{\,2} + \frac{{m_\pi}^2}{2})}, \tag{26}$$

with

$$\widetilde{V}(q) = \widetilde{V}_N(q) + \widetilde{V}_\Delta(q). \tag{27}$$

Here $\widetilde{V}_N(q)$ and $\widetilde{V}_\Delta(q)$ are given by Eqs. (22) and (24) incorporating in the integrand the product $F(\vec{p})F(\vec{p}+\vec{q})$ of Eq. (25). The potential in coordinate space is given by

$$\begin{aligned} V^{(S)}_{NN}(r) &= \int \frac{d^3q}{(2\pi)^3} e^{i\vec{q}\vec{r}} t_{NN}(q) \\ &= \frac{1}{2\pi^2}\frac{1}{r}\int_0^\infty q dq \sin(qr) t_{NN}(q). \end{aligned} \tag{28}$$

We would like to compare $V^{(S)}_{NN}(r)$ with the empirical σ exchange given by

$$V_{NN}^{(\sigma)}(r) = \int \frac{d^3q}{(2\pi)^3} e^{i\vec{q}\vec{r}} \frac{g_{\sigma NN}^2}{-\vec{q}^{\,2} - {m_\sigma}^2}$$
$$= -\frac{g_{\sigma NN}^2}{4\pi} \frac{e^{-m_\sigma r}}{r}, \tag{29}$$

with

$$\frac{{g_{\sigma NN}}^2}{4\pi} = 5.69; \; g_{\sigma NN} = 8.46, \tag{30}$$

from Ref. [1]. This corresponds to the empirical σ exchange when the two pion box diagrams with the intermediate Δ are considered in addition.

Actually, in Ref. [1] a monopole form factor per vertex with $\Lambda_\sigma = 1.7$ GeV is also included so that

$$V_{NN}^{(\sigma)}(q) = -g_{\sigma NN}^2 \left(\frac{\Lambda_\sigma^2 - m_\sigma^2}{\Lambda_\sigma^2 + \vec{q}^{\,2}} \right)^2 \frac{1}{m_\sigma^2 + \vec{q}^{\,2}}, \tag{31}$$

which leads to the potential in coordinate space

$$V_{NN}^{(\sigma)}(r) = \frac{1}{4\pi} g_{\sigma NN}^2 \left\{ \frac{1}{r} e^{-\Lambda_\sigma r} + \frac{\Lambda_\sigma^2 - m_\sigma^2}{2\Lambda_\sigma} e^{-\Lambda_\sigma r} - \frac{1}{r} e^{-m_\sigma r} \right\}, \tag{32}$$

with the same asymptotic behaviour as Eq. (29) at large distances and the finite limit $-(\Lambda_\sigma - m_\sigma)^2/2\Lambda_\sigma$ for $r \to 0$.

4 Qualitative discussion of the potential

Let us go back to Eq. (14) in the physical region. We know from Ref. [16] that the isoscalar amplitude develops a pole around $450 - i225$ MeV. Let us neglect for this study $\mathrm{Im}G(s)$ and rewrite Eq. (14) as

$$t_{\pi\pi\to\pi\pi}^{(I=0)} = \frac{-G(s)^{-1}(s - \frac{{m_\pi}^2}{2})}{s - (\frac{{m_\pi}^2}{2} - f^2 G(s)^{-1})}, \tag{33}$$

so that

$$\frac{{m_\pi}^2}{2} - f^2 G(s)^{-1} \simeq {m_\sigma}^2;\ G(s)^{-1} = \frac{1}{f^2}(\frac{{m_\pi}^2}{2} - {m_\sigma}^2). \tag{34}$$

Assuming now that $G(s)^{-1}$ is a smooth function of s and $\widetilde{V}(q)$ is a smooth function of q, we would have

$$\begin{aligned} t_{NN}(q) &\simeq \widetilde{V}(0)^2 \frac{6}{f^2} \frac{({m_\sigma}^2 - \frac{{m_\pi}^2}{2})(\vec{q}^{\,2} + \frac{{m_\pi}^2}{2})}{\vec{q}^{\,2} + {m_\sigma}^2} \\ &= \widetilde{V}(0)^2 \frac{6({m_\sigma}^2 - \frac{{m_\pi}^2}{2})}{f^2} \frac{(\vec{q}^{\,2} + {m_\sigma}^2) - ({m_\sigma}^2 - \frac{{m_\pi}^2}{2})}{\vec{q}^{\,2} + {m_\sigma}^2}. \end{aligned} \tag{35}$$

We see that the first term in the numerator of the second fraction gives rise to a repulsive δ function in coordinate space, while the second term gives rise to an attractive potential due to a standard σ exchange with the equivalent coupling

$$g_{\sigma NN} \simeq \widetilde{V}(0)\sqrt{6}\frac{({m_\sigma}^2 - \frac{{m_\pi}^2}{2})}{f} \tag{36}$$

With the value $\widetilde{V}(0) \simeq 0.10 \times 10^{-2}$ MeV^{-1} that we obtain, as we shall see, the σNN coupling would be of the order of $g_{\sigma NN} \simeq 5$, which has the right order of magnitude, compared with the empirical coupling used in Ref. [1] to provide the needed intermediate range attraction, $g_{\sigma NN} \simeq 8.5$.

This qualitative study is certainly improved by the accurate results which we give in the next section, but it serves to illustrate the features which we can expect from such a potential. The interesting thing is that, apart from the intermediate attraction, one gets a scalar repulsion, which is also demanded by the NN scattering data.

5 Results and discussion

The qualitative discussion of §4 relies on the constancy of the $G(s)$ function of Eq. (16). This function is rather smooth and is negative in the range of momenta of interest. For $s = 450$ MeV^2 it is about -0.02, and in the range of s from 0 to -500 MeV^2 it varies between -0.02 and -0.015 . The function $\widetilde{V}(q)$ changes slightly faster and drops by a factor of 2 as q varies from 0 to 550 MeV. Hence the qualitative results of that section are only indicative of the actual numerical results.

We performed the calculations using a value of Λ for the monopole form factors of Eq. (25) of 1.1 GeV.

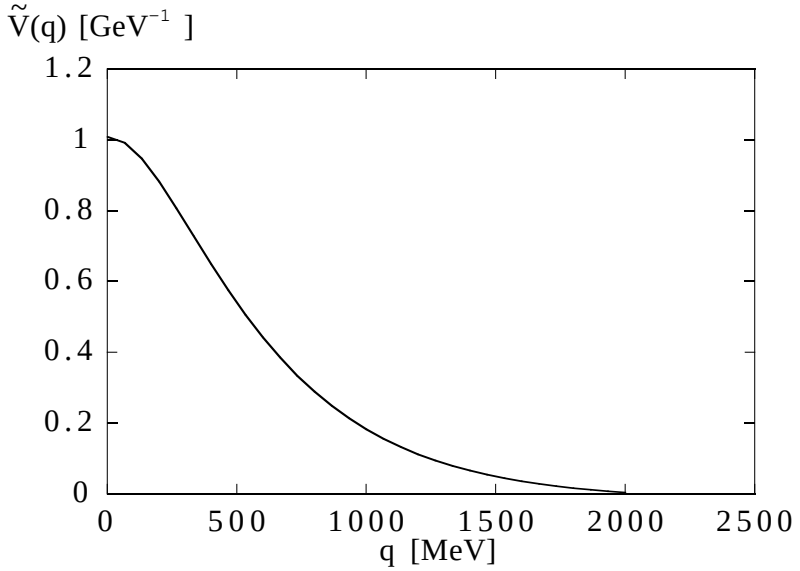

Figure 8: The vertex function $\tilde{V}(q)$ as a function of momentum q.

In Fig. 8 we give the results for the vertex function, which display a moderate but steady decrease of the vertex with q. This ensures convergence of the integral of Eq. (28) for $V(r)$. At this point we note already some discrepency with Ref. [9], where no form factors were used in the evaluation of the vertex function. The divergences obtained there led to singularities at short distances which were disregarded, since only the peripheral NN partial waves were investigated there. In the present case, both the q dependence of the form factor and the extra denominator in Eq. (26) from the iteration of unitary loops, which produces the sigma resonance, improve the convergence properties of the integral of Eq. (28). The function $t_{NN}(q)$ of Eq. (26) is plotted in Fig. 9. It exhibits an increase from 0 to about 500 MeV and then drops as q increases further. For q around 2 GeV, it has a value about 250 times smaller than at the maximum.

We should caution that the unitary theory used here leads to good results in the physical region up to about $\sqrt{s} = 1.2$ GeV. It is then clear that one should not

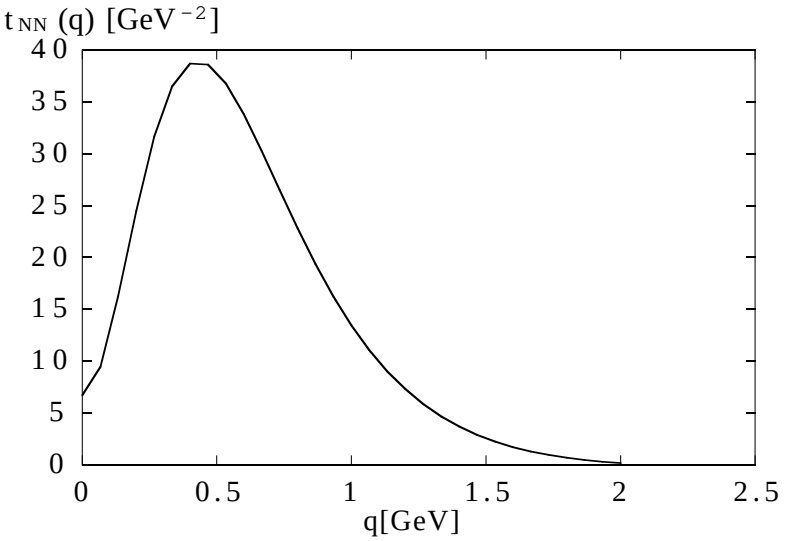

Figure 9: The function t_{NN}.

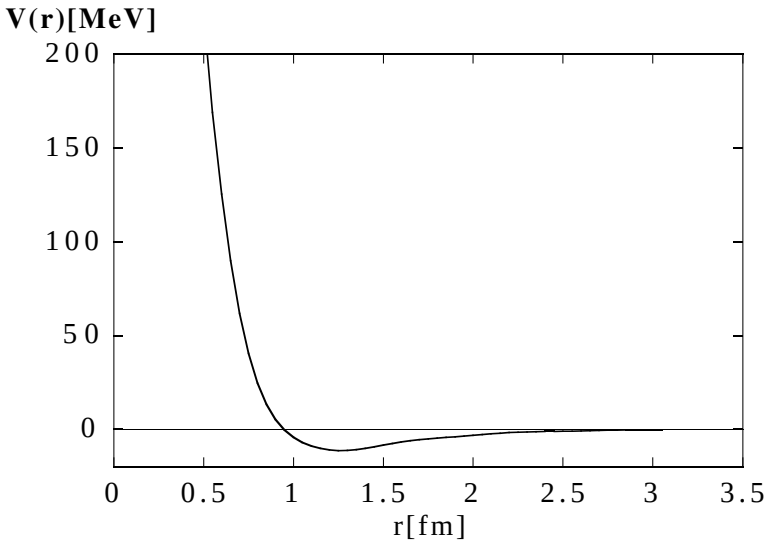

Figure 10: The NN potential in coordinate space

extrapolate the results of the model in the unphysical region to values of q much larger than 1 GeV. In this sense, the form factors in the πNN vertices with lambda of order 1 GeV guarantee that one does not enter into this unknown region. In any case, the uncertainties for these large values of q would revert into uncertainties at

short distances in $V(r)$, which we certainly must admit. Technically, the function $t_{NN}(q)$ of Eq. (26) develops a pole around 2060 MeV, far away from the region of validity of the model used, and to which we do not give any physical meaning. This is anyway a warning that we should not attempt to investigate the behaviour of the potential at very short distances with the present model. The numerical integrations are extended up to 2 GeV in the actual calculations. The predictions for $V(r)$ beyond $r = 0.5$ fm should be rather safe.

In Fig. 10 we show the results for $V(r)$. We find interesting behaviour with a moderate attraction beyond $r = 0.9$ fm and a repulsion at shorter distances, which become of order 1 GeV at very short distances, with the caveat discussed above. Around 0.5 fm it has a value of around 200 MeV. The trend of the results agrees with the qualitative results anticipated in §4. The first thing to note is that these results are quite different qualitatively from those of the conventional sigma exchange, where there is only attraction, according to Eq. (32). They also differ appreciably from those of Ref. [9] where a very weak repulsion is obtained in the region where we find an attraction here (the attraction of the order of eV found numerically at larger distances in Ref.9 is not significative). This finding is relevant since it shows that even for large distances, which is the focus of Ref. [9], one needs to go beyond perturbation theory in the $\pi\pi$ interaction in order to determine the behaviour of the potential. A study of the behaviour of $V(r)$ around 2.5 fm reveals Yukawa behaviour with m_σ around 450 MeV and a coupling $g_{\sigma NN}$ of about 8, in rough agreement with the results of the qualitative discussion of §4, demonstrating that the sigma pole appearing in the physical region shows up indeed in the potential at large distances. Yet, the presence of the sigma pole is not the only element responsible for the behaviour of the potential seen in Fig. 10. Indeed, if we replace the denominator of Eq. (26) by unity, thus removing the sigma pole, we still find structure of the potential similar to that in Fig. 10, with the attraction appearing at shorter distances beyond $r = 0.85$ fm. The strength of the attraction is larger and also falls off faster with increasing r, indicating that the range is now given by other q-dependent functions. In this case, the vertex function and its q dependence are responsible for that behaviour and for the differences with the results of Ref. [9]. Both the vertex function and the unitary approach to the $\pi\pi$ interaction are thus very important for the isoscalar potential and for determining its strength in all ranges of distances. Note that the phenomenological form factor that we assume modulates the structure of the vertex. It not only affects the vertex at large q, in which case only the short range part of the interaction would be modified, but

it also modifies the strength of the vertex at finite q, and this also has influence in the medium and long range parts of the interaction. For similar reasons, the unitarization changes the q dependence, but more importantly it introduces a pole in the s channel, which is reflected in the t channel by a distinct tail in r that goes roughly as $e^{-m_\sigma r}/r$.

The evaluation of the vertex function here has been done using elements of phenomenology, beyond the chiral approach otherwise used. In this sense the monopole form factors were used and the space of intermediate baryon states was truncated in the delta. Other more realistic options could be used, maybe even using form factors obtained within the chiral approach in some self-consistent way. For the time being we should admit uncertainties from this source.These uncertainties should not be minimized since the results depend appreciably on the choice of the range parameters. For instance a change of lambda from 1.1 GeV to 1.2 GeV changes the attraction from 10 to 15 MeV. A different vertex evaluation, in which an explicit contribution of states beyond the delta in the intermediate states is allowed, as in Ref. [22] would also lead to different q behaviour of the vertex function, with immediate results in the potential in coordinate space. The regularization procedure can be done in many ways. In chiral perturbation, it requires a regularization scheme by means of a regularization scale or a cut-off, but at the same time one has to introduce counter-terms of higher order. In the case of the meson-meson interactions, it is proved in Ref. [17] and [20] that a cut-off, or equivalently dimensional regularization at a certain scale, effectively generates the counter-terms in the meson-meson s-wave channel. For the vertex functions, which we generate here, such a procedure is not yet available. In Ref. [8] and [9], infinities in the vertex function are removed with the claim that this removal affects only the short range part of the interaction. In our case we have resorted to phenomenology using an empirical πNN form factor which makes the loop function convergent. The fact that with this procedure we find an assymptotic behavior for the potential similar to the empirical σ potential gives us confidence that this "empirical" regularization in the baryon sector is a reasonable procedure.

In any case, given all the limitations which have been discussed above, we can not make strong claims about the strength of this σ potential, but we certainly can stress the qualitative features, which are rather different from the conventional results for sigma exchange and from results obtained in the perturbative approach to the problem.

6 Conclusions

We have evaluated the contribution to the NN potential from the exchange of an interacting pion pair in the scalar-isoscalar channel, the sigma channel. We have used a unitary model based upon the lowest order chiral Lagrangian and the Bethe-Salpeter equation. This model is supported by a more elaborate approach using the inverse amplitude method and the lowest and second order chiral Lagrangians, but technically simpler. Both approaches generate a sigma pole around 450 MeV, although with a large width. The $\pi\pi$ amplitude extrapolated to negative values of s, retains memory of the sigma pole and leads to a tail of the NN potential reflecting a Yukawa behaviour with the range of the sigma mass. We obtain some moderate attraction beyond 0.9 fm and a stronger repulsion before that. This behaviour is quite different from that of the conventional sigma exchange, which always leads to an attractive force, even in the presence of form factors for the σNN vertices.

We have also found that the procedure chosen to regularize the σNN vertex function also has important consequences for the potential. We have chosen to introduce phenomenological form factors for the πNN vertices and to restrict the space of baryon intermediate states in the loop to the nucleon and the delta, a procedure which has been often used in related problems in connection with chiral quark models. The results are sensitive to the form factors and the manner in which the vertex is constructed. This is one of the problems that requires further thought. For the moment, we should accept one degree of freedom due to the divergence of the vertex loop, which must be cured with some regularization mass, a counterterm, the use of a form factor, etc. We can hope to reduce the freedom by using some empirical information, as in the present case . Hence we believe our results are qualitatively acceptable in the range of distance beyond 0.5 fm, and more quantitatively accurate results. The findings of this paper are important because they reveal behaviour that is quite different from that which one gets from the conventional sigma exchange picture. On the other hand, it is also known that a nonperturbative approach to the $\pi\pi$ interaction is needed, and such an approach should be important for obtaining proper results in the whole range of distances in the NN interaction. These findings should thus have important consequences in the chiral approach to the NN interaction, which is now the subject of much theoretical investigation.

Acknowledgements

We are grateful to the COE Professorship program of Monbusho, which enabled E. O. to stay at RCNP to perform the present work. One of us, E. O., wishes to thank N. Kaiser for useful discussions. This work is partly supported by DGICYT contract number PB96-0753.

References

[1] R. Machleidt, K. Holinde and Ch. Elster, Phys. Rep. **149** (1987), 1.

[2] J. W. Durso, A. D. Jackson and B. J. Verwest, Nucl. Phys. **A345** (1980), 471.

[3] R. A. Smith and V. R. Pandharipande, Nucl. Phys. **A256** (1976), 327.

[4] A. M. Green, Rep. Prog. Phys. **39** (1976), 327.

[5] J. Gasser and H. Leutwyler, Ann. of Phys. **158** (1984), 142; Nucl. Phys. **B250** (1985), 465, 517, 539.

A. Pich, Rep. Prog. Phys. **58** (1995), 563.

G. Ecker, Prog. Part. Nucl. Phys. **35** (1995), 1.

U. G. Meissner, Rep. Prog. Phys. **56** (1993), 903.

[6] C. Ordonez, L. Ray and U. van Kolck, Phys. Rev. **C53** (1996), 2086.

[7] D. B. Kaplan, M. J. Savage and M. B. Wise, Nucl. Phys. **C478** (1996), 629; Phys. Lett. **B424** (1998), 390.

[8] N. Kaiser, R. Brockmann and W. Weise, Nucl. Phys. **A625** (1997), 758.

[9] N. Kaiser, S. Gerstendörfer and W. Weise, Nucl. Phys. **A637** (1998), 395.

[10] C. Caso, Eur. Phys. J. **C3** (1998), 1.

[11] B. S. Zou and D. V. Bugg, Phys. Rev. **D48** (1993), 3948.

[12] M. Roos and N. A. Tornqvist, Phys. Rev. Lett. **76** (1996), 1575.

[13] M. Y. Ishida, Nucl. Phys. **A629** (1998), 148c.

[14] G. Janssen, B. C. Pearce, K. Holinde and J. Speth, Phys. Rev. **D52** (1995), 2690.

[15] T. N. Truong, Phys. Rev. Lett. **61** (1988), 2526; **67** (1991), 2260.
A. Dobado, M. J. Herrero and T. N. Truong, Phys. Lett. **B235** (1990), 134.
A. Dobado and J. R. Peláez, Phys. Rev. **D47** (1993) 4884; **D56** (1997), 4193.

[16] J. A. Oller and E. Oset, Nucl. Phys. **A620** (1997), 438; **A624** (1999) 407, erratum

[17] J. A. Oller, E. Oset and J. R. Peláez, Phys. Rev. Lett. **80** (1998), 3452.

[18] J. A. Oller and E. Oset, Phys. Rev. **D60** (1999), 074023.

[19] U. G. Meissner, E. Oset and A. Pich, Phys. Lett. **B353** (1995), 161.

[20] J. A. Oller, E. Oset and J. R. Peláez, Phys. Rev. **D59** (1999), 74001.

[21] E. Jenkins, Nucl. Phys. **B368** (1992) 190; Phys. Lett. **B325** (1993), 431.
A. V. Manohar, Phys. Lett. **B336** (1994), 502.

[22] E. Oset, Nucl. Phys. **A411** (1983), 357; **A430** (1984), 713.

[23] A. W. Thomas, S. Theberge and G. A. Miller, Phys. Rev. **D24** (1981), 216.
A. W. Thomas, Adv. Nucl. Phys. **13** (1983), 13.